Effects of fluid distribution and subsurface structural heterogeneity on ground-penetrating radar

Michael B. Kowalsky[1], Yoram Rubin[1] and Peter Dietrich[2]
[1]Dept. of Civil and Environmental Engineering, U. of California, Berkeley, CA 94720; MBKowalsky@lbl.gov
[2]Dept. of Applied Geology, U. of Tuebingen, 72076 Tuebingen, Germany

1.0 Introduction

There is a great need for improved shallow subsurface characterization tools, with the motivation being, for example, to monitor water content in agricultural applications, or to predict the transport of contaminants through the vadose zone and into the groundwater (e.g., Foussereau et al., 2001; Russo et al., 2001). In the right conditions geophysical tools, such as ground-penetrating radar (GPR), can be helpful to assist in characterizing sedimentary environments and constructing contaminant transport models. Two popular configurations for data collection are: surface surveys in which time series of reflections are recorded at the surface; and crosshole tomography in which spatial distributions of velocity and attenuation may be obtained between boreholes. Surface and crosshole GPR are fitting for the characterization of sedimentary environments if the sedimentary units are characterized by distinct electrical properties. Studies where GPR was successfully used to map sedimentary structures revealed that lithologic units often have varying electrical properties which enables their detection (e.g., Vandenberghe, J., and R. A. van Overmeeren, 1999; Beres et al., 1999). However, the factors which make some structures visible, and others not, is an area of active research.

Outcrop analog studies have been helpful for assessing the suitability of geophysical methods and for the overall investigation of contaminant transport scenarios. Outcrop derived models have been used to test transport model generation algorithms (Whittaker and Teutsch, 1999), and also to gain insight by revealing relevant sedimentary structures which govern contaminant transport (Klingbeil, 1998; Kleineidam, 1999). Outcrop analogs have also been used to test geophysical tools in attempt to better understand what is measured in GPR surveys (van Dam and Schlager, 2000; Tronicke, 2001). Through such outcrop analog studies, it has also been noted that the electrical parameters that govern GPR wave propagation depend not only on sedimentological units but are also highly sensitive to the presence of water, the amount and location of which may of course vary with time. GPR images are then expected to vary significantly with the state of water saturation, as was suggested, for example, in an outcrop modeling study where the occurrence of reflections in a GPR image depended on a heterogeneous distribution of pore water (Kowalsky et al., 2001).

It is also well known that water content in the vadose zone can vary with time. The sensitivity of GPR to the presence of water might be exploited in the case where the electrical properties of subsurface targets vary significantly due to transients in water content, such as for open-framework gravel layers, which can serve as conduits for flow in the saturated zone and tend to drain faster than the fine grained materials surrounding them. Taking advantage of heterogeneous time-varying water distributions should help in obtaining additional information about subsurface structure and obtaining improved maps of sedimentary units. Time-lapsed measurements have in fact been shown to offer useful information, for example, to help identify the location of a (moving fluid) target such as DNAPL (Brewster and Annan, 1994), and to help visualize soil moisture patterns (Eppstein and Dougherty, 1998). But to better understand time-lapsed GPR data in the vadose zone, it is necessary to further consider fluid flow processes.

In previous work, simplified distributions of water content were assumed in order to simulate GPR in an outcrop model (Kowalsky et al., 2001). In the present study we simulate unsaturated flow and GPR surveys simultaneously using an outcrop analog model to investigate the response of GPR during various hydrologic events such as wetting and drying cycles in the subsurface. This enables the investigation of time-lapsed GPR data for an improved characterization of the subsurface. The simulation of different GPR acquisition techniques during different stages of water saturation will allow for the evaluation of GPR for

different goals including the construction of contaminant transport models, the monitoring of water content for agriculture, and the overall characterization of sedimentary environments.

2.0 Outcrop Modeling Study

The field site being modeled in this study is at a gravel quarry in the city of Herten, Germany. Sedimentary deposits in this region were formed in a braided river environment and consist mainly of layers of poorly to well-sorted sand and gravel with no silt or clay. During the summer of 1999, an outcrop analog project was performed in which geophysical data were first collected, and the site was then excavated in increments of 1-2 meters such that photographs of the advancing outcrop face could be taken and later converted to lithologic maps. Outcrop images corresponding to the planes of the GPR surveys were then available. This enabled the comparison of observed GPR reflections to the actual lithology images (Bayer, 2000), and it also enabled the construction of models for the simulation of GPR under varied subsurface conditions (Kowalsky et al., 2001). In the latter study, it was shown that for synthetic GPR to exhibit the main features in field data, a model with non-uniform water saturation was required. But, to obtain a non-uniformly saturated model some simplified assumptions were made regarding the distribution of water in the various lithologic units: the open-framework gravel units were assumed to be more drained than the surrounding units; and water content was assumed to be constant and uniform throughout each lithologic unit. In the present study, TOUGH2 (Pruess, 1991) is used to simulate non-steady state infiltration at the Herten site using the aforementioned outcrop model. For several times during infiltration, GPR is simulated using a finite-difference code, and the impact of non-uniform time-varying water saturation on GPR data is investigated. The modeling procedure for a 1D column from this outcrop and some preliminary results will next be described.

Simulating infiltration

In order to simulate infiltration in the vadose zone, van Genuchten parameters typical for course sands were chosen (van Genuchten, 1980; Pruess, 1996), and the capillary strength was scaled by the permeability measured for each lithologic unit (e.g., Warrick et al., 1977). A grid size of 5 cm was used for a model extending 6 meters in depth. Atmospheric conditions were held at the top of the model. And since the water table is know to have been below the bottom of the outcrop, water saturation was held constant at the bottom of the model at a value of 0.7. Before simulating the infiltration experiment, 'natural' conditions were obtained (i.e., gravity-capillary equilibrium) by simulating flow for 90 years with the aforementioned boundary conditions and arbitrary initial conditions until the system was approximately at steady state. Then an infiltration experiment was simulated by placing a constant water head of 5 cm at the upper boundary for 30 minutes. Following this, atmospheric conditions were returned to the surface and the water distribution was observed for increasing times.

The distribution of water within the modeled column is shown for several times in Figure 1a. The well known phenomenon of water ponding is observed above the partially saturated open frame-work gravel layers, which are indicated by regions of gray shading (Figure 1-2). In contrast, water content below these gravel layers is much lower and drains more quickly with time. This trend forms the basis for understanding the time-varying change in electrical properties and as will be shown, might allow for the delineation of such open frame-work gravel layers with geophysical methods. It is also useful to note that the location of such capillary barriers is important (i.e., the distance to underlying capillary barrier affects rate of drainage). The relative change in water content is shown in Figure 1b. And the model permeability distribution is shown in Figure 1c.

2D flow modeling is also being performed and additional variations in water content associated with 2D flow phenomena are observed. For example, the inclination of the gravel layers affects the rate of ponding/drainage and directs water laterally. The simulation of GPR during the aforementioned synthetic infiltration experiment is next described.

Simulating GPR during infiltration

In order to simulate GPR, the electrical properties were estimated for each lithological unit using petrophysical models (see Kowalsky et al [2001] for a more detailed description). The EM velocity distribution for three times after the simulated infiltration is shown in Figure 1a, and the relative change in velocity from 1 week to 6 months after infiltration is shown Figure 2b. Among other factors, EM velocity is inversely proportional to water content (Figure 1a) and proportional to porosity (Figure 2c). This explains why the high porosity open-framework gravel (at low saturation) have higher velocity, whereas, the regions above gravel layers with increased water content due to ponding have lower velocity. Changes in velocity with time above the open frame-work gravel layers are small, whereas changes in velocity below are relatively large. One instance where this trend is not apparent is between the first two gravel layers (both located between 1 and 2 m depth); the second gravel layer is so close to the first that ponding above the second layer is already occurring directly below the first layer.

A finite difference time-domain (FDTD) code was used to simulate GPR for various data acquisition geometries at different times during drainage (e.g., Bergmann et al., 1994). An example is shown in Figure 3, where a time-lapsed GPR surface reflection survey was simulated for a source frequency of 250 MHz. The electrical parameters were calculated for two times during drainage, and the impact on the traces of the changing water content can be seen. In this case, the reflection time is the most notable change from one time to the next; a maximum travel time increase of 1-2 ns is seen. This is because certain regions are dryer and, therefore, have a higher velocity than when they are wetter. The average velocity of both velocity distributions was used to convert reflection time to approximate depth to allow comparison between the model and GPR reflections (travel time is shown on the top axis in Figure 3, approximate depth on the bottom axis). Although the changes in travel time and amplitude observed in this case are small, changes in amplitude are more pronounced when the infiltration front is passing through the model (not shown).

Averaging the 1D velocity models can be performed to gain an insight into the impact of transient water content on tomographic data. This is done by calculating the average values with averaging lengths equal to the resolution of the GPR surveys (100 MHz and 250 MHz are assumed). The 1D velocity models are shown in Figure 4a-b and represent ideal vertical slices from crosshole tomograms obtained during infiltration. These plots demonstrate 1) the smoothed nature of tomographic data (i.e. it is not always possible to image the open-framework gravel layers directly), 2) the improved resolution of targets with increased GPR frequency, and 3) that time lapse tomographic data should be sensitive to changes in velocity which are caused by differential draining above and below open frame-work gravel layers (see Figure 4c). This may provide a way to delineate open-framework gravel. For example, the water content changes only 1% above the gravel layer at 2.4m for this case, whereas the water content changes nearly 5% below that gravel layer.

Sensitivity of the results to parameter variability (variability within lithologic units as well as between individual units) is also being investigated. And it is important to note that changes in water content seen in this 1D model are sensitive to boundary conditions. The 2D simulations which are being performed will yield actual tomograms for more precise analysis.

3.0 Conclusions and Future Research

It is well known that GPR is sensitive to water content, and that water content is often non uniform (between and within lithologic units). This should be considered while interpreting GPR data. In addition to being related to soil type, water content in the vadose zone is of course also related to the sequence of hydraulic properties such as the permeability. During transient flow events like infiltration and drying cycles, the distribution of water content in the subsurface also varies with time. We present some forward modeling results in which the sensitivity of GPR to transient fluid flow in an outcrop model is investigated. In this manner, we aim to better understand the relation between fluid flow processes and GPR data. Since GPR has the potential, as shown, to measure changes in water saturation, which are

related to permeability structure, we aim to use GPR data to infer permeability structure in the subsurface (e.g., using time-lapsed GPR data in conjunction with hydraulic data for hydraulic parameter inversion).

Acknowledgements

References

Bayer, P., Aquifer-Anolog-Studie in grobklastischen 'braided river' Ablagerungen: Sedimentaere/ hydrogeologische Wandkartierung und Kalibrierung von Georadarmessungen, Diplomkartierung, Universitaet Tuebingen, 2000.

Beres, M., P. Huggenberger, A. Green and H. Horstmeyer, 1999. Using two- and three-dimensional georadar methods to characterize glaciofluvial architecture, *Sedimentary Geology*, 129, 1-24.

Bergmann, T., J. O. A. Robertsson, and K. Holliger, Finite-difference modeling of electromagnetic wave propagation in dispersive and attenuating media: *Geophysics*, 63(3), 856-867, 1998.

Brewster, M. L., and A. P. Annan, Ground-penetrating radar monitoring of a controlled DNAPL release: 200 MHz radar, *Geophysics*, 59(8), 1211-1221, 1994.

Eppstein, M. J., and Dougherty, D. E., Efficient three-dimensional data inversion: Soil characterization and moisture monitoring from cross-well ground-penetrating radar at a Vermont test site, *Water Resour. Res.*, 34(8), 1889-1900, 1998.

Foussereau, X., W. D. Graham, G. A. Akpoji, G. Destouni, P. S. C. Rao, Solute transport through a heterogeneous coupled vadose-saturated zone system with temporally random rainfall, *Water Resour. Res.*, 37 (6), 1577-1588, 2001.

Kleineidam, S., H. Ruegner, B. Ligouis, and P. Grathwohl, Organic matter facies and equilibrium sorption of phenanthrene. *Environ. Sci. and Technol*. 33, 1637-1644, 1999.

Klingbeil, R., 1998. Outcrop Analog Studies: Implications for groundwater flow and Contaminant Transport in Heterogeneous Glaciofluvial Quaternary Deposits, Ph.D. Dissertation, University of Tuebingen, Germany, 1998.

Kowalsky, M. B., P. Dietrich, G. Teutsch, and Y. Rubin, Forward modeling of ground-penetrating radar data using digitized outcrop images and multiple scenarios of water saturation, *Water Resour. Res.*, 37(6), 1615-1625, 2001.

Pruess, K., TOUGH2—A general purpose numerical simulator for multiphase fluid and heat flow. Report No. LBL-29400, Lawrence Berkeley National Laboratory, Berkeley, CA, May, 1991.

Pruess, K., A Fickian diffusion model for the spreading of liquid plumes infiltrating in heterogeneous media, *Transport in Porous Media*, 24(1), 1996.

Russo, D., J. Zaidel, A. Laufer, Numerical Analysis of flow and transport in a combined heterogeneous vadose zone—groundwater system, *Advances in Water Resources*, 24, 49-62, 2001.

Tronicke, J., Improving and evaluating GPR techniques for subsurface characterization: case strategies and advanced analysis strategies, Ph.D. Thesis, University of Tuebingen, Germany, 2001.

van Dam, R. L., and W. Schlager, Identifying causes of ground-penetrating radar reflections using time-domain reflectometry and sedimentological analyses, *Sedimentology*, 47, 435-449, 2000.

van Genuchten, M. Th., A closed-form equation for predicting the hydraulic conductivity of unsaturated soils, *Soil. Sci. Soc. Am. J.* 44, 892-898, 1980.

Vandenberghe, J., and R. A. van Overmeeren, Ground penetrating radar images of selected fluvial deposits in the Netherlands, *Sedimentary Geology*, 128, 245-270, 1999.

Warrick, A. W., G. J. Mullen, and D. R. Nielsen, Scaling Field-Measured Soil Hydraulic Properties Using a Similar Media Concept, *Water Resour. Res.*, 13(2), 355-362, 1977.

Whittaker, J., and G. Teutsch, Numerical simulation of subsurface characterization methods: application to a natural aquifer analogue: *Advanced in Water Resources*, Vol. 22, No. 8, 819-829, 1999.
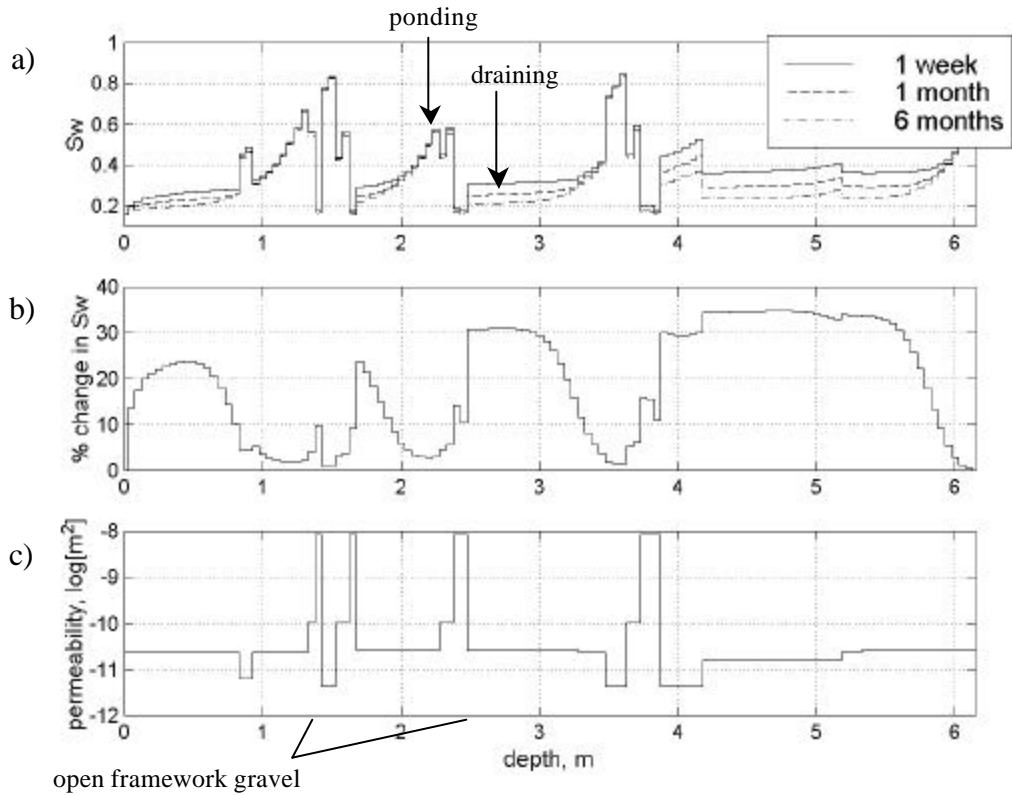
Figure 1: 1D Simulation of drainage (following infiltration). The distribution of water saturation (Sw) with depth is shown (a) with increasing time after an infiltration event (5cm ponding infiltration for 30 minutes). The relative change in Sw from 1 week to 6 months is shown in (b). The infiltration simulation is based on the permeability distribution shown in (c).
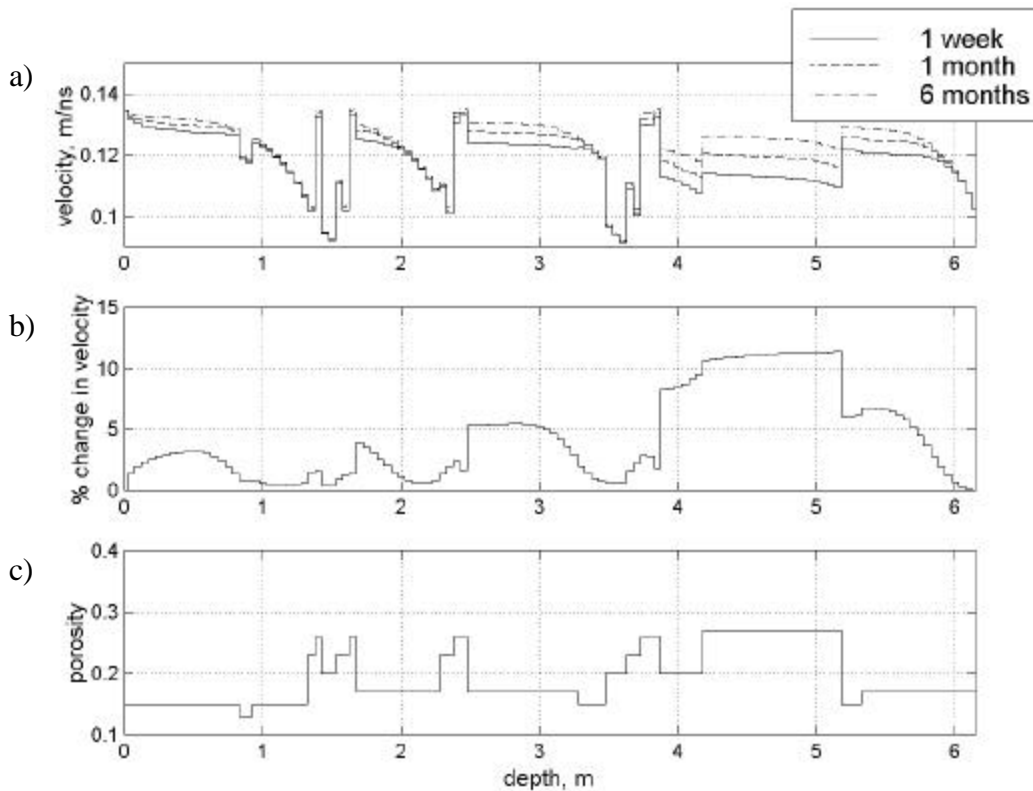

Figure 2: Electromagnetic (EM) wave velocity during drainage are shown (a) for increasing times during drainage. The relative change in EM velocity from 1 week to 6 months is shown in (b). The porosity values shown in (c) and the Sw values (Figure 1a) were used to calculate the EM velocity values in (a).
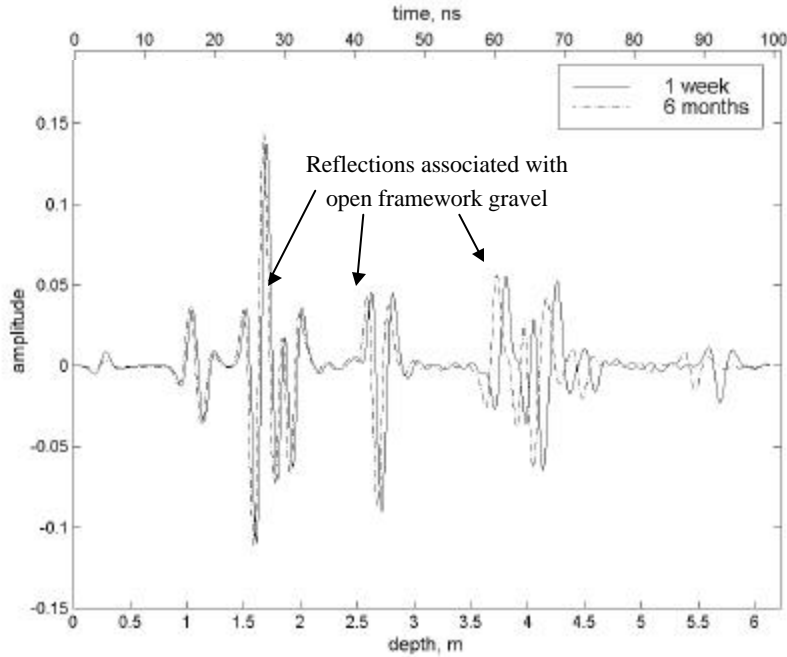
Figure 3: Surface reflection GPR survey (FDTD simulation) for two times during drainage. The average velocity was used to convert GPR travel time (top) into approximate reflection depth (bottom).
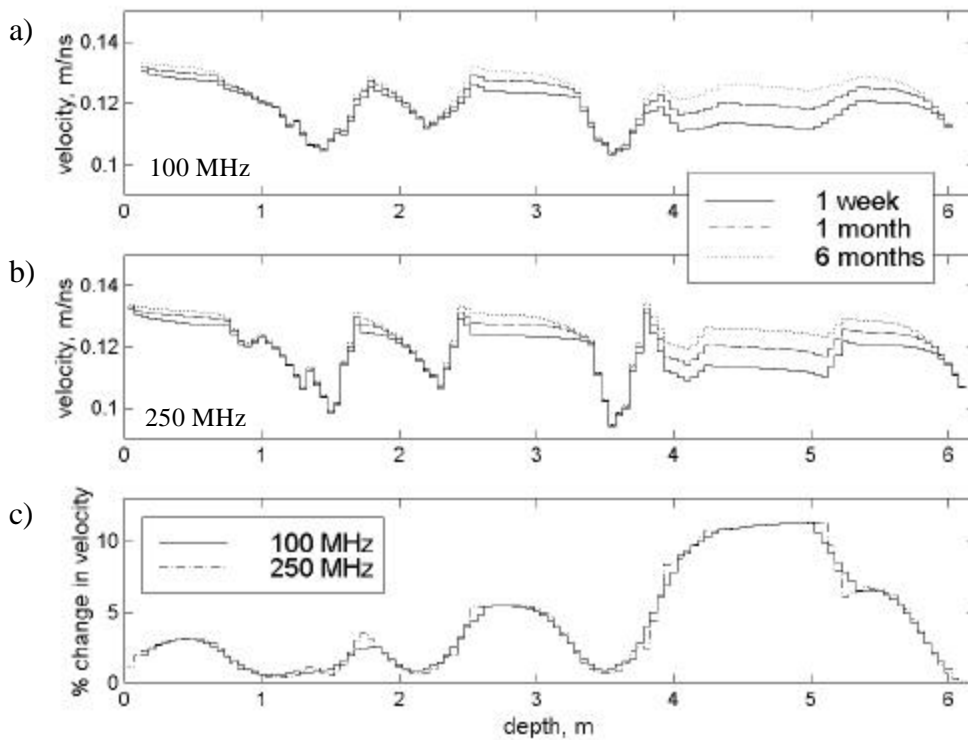

Figure 4: EM velocity averaged with a moving window corresponding to the resolution of GPR crosshole surveys. The velocity distributions in (a) and (b) represent vertical slices from GPR crosshole tomograms with frequencies of 100 MHz and 250 MHz, respectively. The relative changes in velocity from 1 week to 6 months are shown in (c).